Effect of Unit Cement Content on Surface Deterioration and Corrosion of Rebar Suffering Combined Chloride-Induced Deterioration and Frost Damage

Yuriko YAMAMOTO[1*], Hiroshi YOKOTA[2], Katsufumi HASHIMOTO[2] and Yuta JOHGASAKI[1]

[1]*Graduate School of Engineering, Hokkaido University, Japan*
[2]*Faculty of Engineering, Hokkaido University, Japan*
Kita 13, Nishi 8, Kita-ku, Sapporo,Hokkaido 060-8628, Japan,
yurincorhcp14@ec.hokudai.ac.jp, yokota@eng.hokudai.ac.jp,
hashimoto.k@eng.hokudai.ac.jp, johgasaki@eng.hokudai.ac.jp

ABSTRACT

It is known that higher unit cement content provides higher strength and less scaling of frost damaged concrete.   Moreover, higher unit cement content is expected to have less chloride ion movement and higher binding capacity against chloride-induced deterioration.   When deterioration progress of concrete in cold regions is discussed, chloride attack and frost damage should be considered simultaneously because deicing agents that may accelerate the combined deterioration are widely spread.   In this study, the influence of unit cement content on the combined deterioration of chloride-induced deterioration and frost damage is experimentally investigated.   During the freezing-thawing experiment of reinforced concrete partly submerged into artificial seawater, scaling depth and volume, total and soluble chloride ion contents, and half-cell potential were measured.   As the results, though higher unit cement content with less aggregate content caused more scaling, higher chloride ion binding capacity could inhibit corrosion of steel rebar under the freezing-thawing environment.

Keywords.   Chloride ion penetration, Frost damage, Scaling, Concrete cover, Unit cement content

INTRODUCTION

Frost damage is one of the principal deterioration phenomena of concrete structures in cold regions.   Deterioration evaluation on the frost damage is based on visual investigation with using the scaling depth and volume and the exposed aggregate ratio as an index of the deterioration.   Furthermore, chloride supplied from deicing agents has to be considered for the evaluation.   Therefore, to properly evaluate deterioration of concrete structures under freeze-thaw environment, it is necessary to investigate multiple deterioration such as frost damage, chloride ion penetration, and corrosion of steel rebar.   A chloride threshold value for initiating rebar corrosion is used to for the prediction of the onset of corrosion due to

chloride attack, which is specified as 1.2 kg/m^3 according to JSCE Standard Specifications for Concrete Structures -2007 Design.   Although there have been some cases in which actual threshold values vary depending on several conditions including mix proportions of concrete.   For example, the chloride threshold value depends on chloride ion binding capacity of cement matrix determined by hydration products (Ishida, et al. 2007).   Consequently, there are some suggestions to determine the chloride threshold value as a function of the unit cement content of concrete (Kono, et al. 2006).

In this study, the influence of unit cement content on the combined deterioration due to freezing-thawing and chloride attack was experimentally investigated by measuring concrete scaling volume and depth, half-cell potential of steel rebar and total, and soluble chloride ion contents.

EXPERIMENT

Test specimens.   Mix proportions of concrete are presented in Table 1, and compressive strengths of concrete are summarized in Table 2.   Slump and air contents of C300 were 10 cm and 6 % respectively, while those of the others were not measured due to slight segregation.   Materials used for the concrete are ordinary Portland cement (C), river sand (S), and crushed stone (G).   In this study, the unit cement contents were varied as 300, 400 and 500 kg/m^3.   The test specimen measured 100 mm × 100 mm × 160 mm.   A deformed steel rebar of 10 mm in diameter was embedded at an angle to vary concrete cover gradually in the specimen (Kono, et al. 2006 and 2010) as shown in Figure 1.   The specimens were cured in water for 28 days and then stored in air for 21 days, followed by pre-water absorption for 7 days prior to the exposure test.

Freezing and thawing test.   The freeze-thaw cycle is shown in Figure 2.   The bottom surface of the specimen was focused during the test.   As shown in Figure 1, the specimen was submerged in sodium chloride solution (3 mass %) up to 5 mm from the bottom surface. The lateral sides were sealed with silicon resin to isolate from the environmental action.

At every 20 cycles, the specimens were taken out from the test chamber and placed in the air for 1 day, followed by the measurement of scaling volume and depth and half-cell potential of rebar.   After the measurement, the specimens were put back into the test chamber with refilled sodium chloride solution (3 mass %).   The specimens after the freezing and thawing test with sodium chloride solution were designated as FTC and those placed in the room kept at 20 °C with sodium chloride solution were designated as NON-FTC.

Measurement.   At every 20 cycles, volume of the FTC specimens was measured.   The scaling volume is a calculated value obtained by dividing the amount of mass loss of the specimens by their surface area.   The scaling depth is a calculated value dividing the scaling volume by the density of the specimen.

Table 1. Mix proportion of concrete

	W/C	s/a	Unit content (kg/m^3)			
	(%)	(%)	W	C	S	G
C300	50	50	150	300	1008	1045
C400	50	60	200	400	1078	746
C500	50	70	250	500	1105	491

Table 2. Compressive strength of concrete

	Compressive strength (N/mm^2)
C300	36.6
C400	41.1
C500	42.8

Table 3. Visual assessment rating (ASTM C 672)

Rating	Condition of surface
0	No scaling
1	Very slight scaling (3 mm depth, max, no coarse aggregate visible)
2	Slight to moderate scaling
3	Moderate scaling (some coarse aggregate visible)
4	Moderate severe scaling
5	Severe scaling (coarse aggregate visible over entire surface)
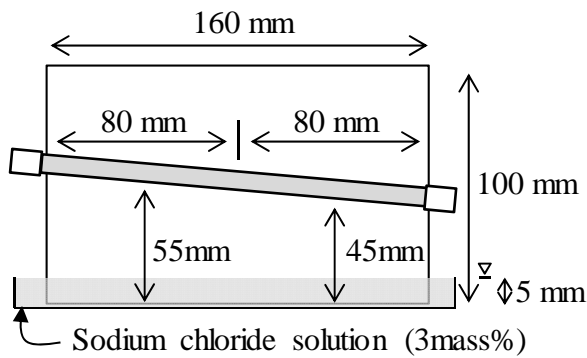
Figure 1. Test specimen and test-setup
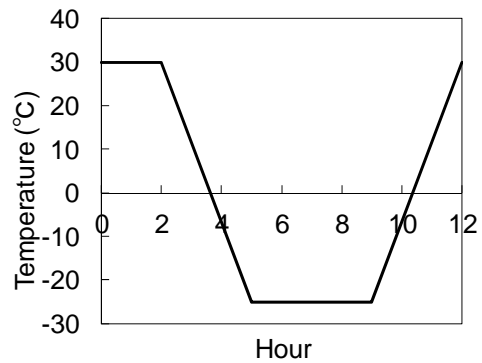
Figure 2. Freeze-thaw cycle
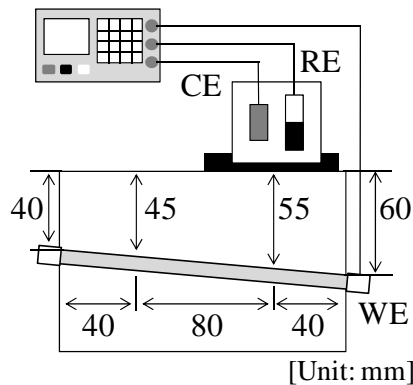
Figure 3. Three-electrode method for measuring half-cell potential

At 60 and 140 cycles, visual assessment of the FTC specimens was conducted according to the ASTM C 672 rating as presented in Table 3. This assessment is a semi-quantitative evaluation focusing on the exposure of coarse aggregate from the surface of the specimen (Hayashida, et al. 2010).

At every 20 cycles, half-cell potential of steel rebar was measured by the three-electrode method as shown in Figure 3 with a portable steel corrosion diagnosis device.   This method consists of a working electrode of steel rebar (WE), a reference electrode of measuring the potential (RE), and a counter electrode of current flows (CE).   During the measurement, the tested surface of the specimens, on which scaling occurred, was kept in wet.   The half-cell potentials were measured at two points with different concrete covers; that is, at the shallow point (45 mm cover) and at the deep point (55 mm cover).

At 60 and 140 cycles, the specimen was cut into 8 slices of 10 mm thick each from the bottom.   Total and soluble chloride contents were measured according to JIS A 1154.

RESULTS AND DISCUSSIONS

Scaling volume and depth.   The scaling volume and the scaling depth are shown in Figures 4 and 5, respectively.   The scaling depth in this study is an imaginary index to identify the degree of scaling when it occurs in a depth direction from the surface.   In these figures larger cement content increased the scaling volume.   This is because scaling is caused by freezing of water in concrete (Kamata, 1988).   Larger cement content leads to the larger cement paste volume concrete in this study, which indicates larger water absorption.

Visual assessment.   The appearances of the specimens deteriorated by frost damage after 140 cycles are shown in Figure 6.   Surface condition was rated according to Table 3 after the freezing and thawing test, which is shown in Figure 7.   The ratings have no differences with unit cement content though the scaling volume is different.

Half-cell potential.   Half-cell potentials of FTC and NON-FTC are shown in Figures 8 and 9, respectively.   The probability of steel rebar corrosion in concrete according to ASTM C876 is presented in Table 4.

In the case of FTC, the half-cell potential fell below the ASTM threshold value in initial cycles.   At 60 and 140 cycles, the steel rebars were taken out from the specimens to evaluate the corrosion condition.   There were no corrosion observed.   The relationship between corrosion rate of steel rebar and temperature is shown in well known Equation (1) (Otsuki, et al. 2004) that has been derived from Arrhenius Equation (2).
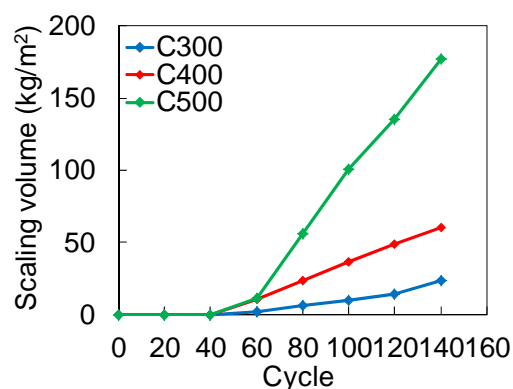
Figure 4. Scaling volume   **Figure 5. Scaling depth**
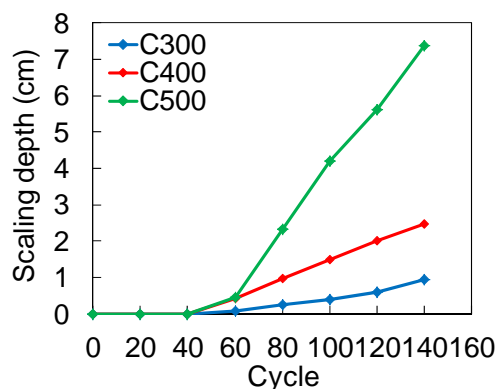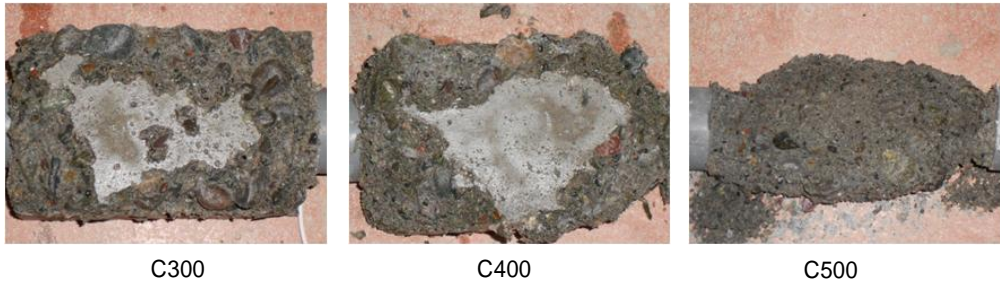
Figure 6. Appearance of the specimens at 140 freeze-thaw cycles
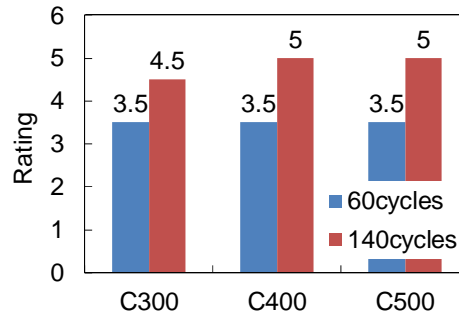
Figure 7. Rating of surface condition

$$\log V = -A\frac{1}{T} + B \tag{1}$$

$$k = \frac{V}{C} = a \exp\left(-\frac{E}{RT}\right) \tag{2}$$

$$A = \log\frac{E}{R}, \quad B = \log C \tag{3}$$

where V is the reaction rate, k is the reaction rate constant, C is the reactant concentration, a is the frequency factor, E is the activation energy, R is the gas constant, and T is the absolute temperature.

In this study, it was confirmed that corrosion rate is low because the specimens are placed in low temperature for the case of FTC. There were no differences among the half-cell potentials with different concrete covers in Figure 8. The reason is considered that the corrosion current does not flow linearly from the counter electrode to the steel rebar due to the surface roughness of the specimens after scaling occurs.

Chloride ion concentration. Distributions of total and free chloride contents and the fixing ratios are shown in Figure 10. The relationship between soluble chloride and free chloride contents is shown in Equation (4) (Ishida, et al. 2007). In this study, the free chloride content was calculated by Equation (5) derived from Equation (4). The fixing ratio was calculated with fixed, total and free chloride contents by Equations (6) and (7). The data at 0.5 cm and 1.5 cm deep in case of C500 were not obtained due to scaling at 140 cycles.

$$C_{sol} = 2.07 C_{free}^{0.55} \tag{4}$$

$$C_{free} = \left(\frac{C_{sol}}{2.07} \right)^{\frac{1}{0.55}} \tag{5}$$

$$C_{fix} = C_{total} - C_{free} \tag{6}$$

$$\lambda = \frac{C_{fix}}{C_{total}} \tag{7}$$

where C_{sol} is the soluble chloride content, C_{free} is the free chloride content, C_{fix} is the fixed chloride content, C_{total} is the total chloride content, and λ is the fixing ratio.
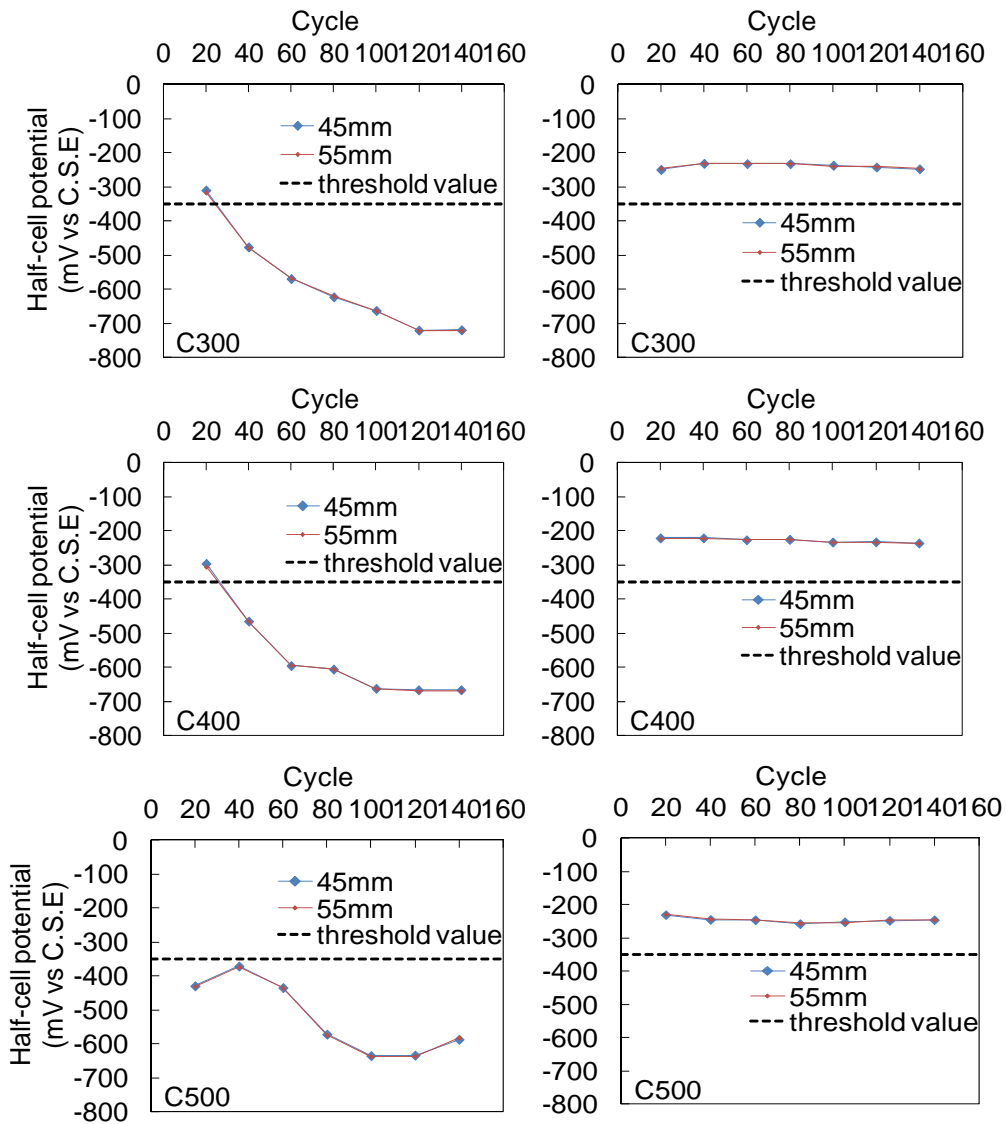
Figure 8. Half-cell potential (FTC)

Figure 9. Half-cell potential (NON-FTC)

Table 4. Probability of steel rebar corrosion (ASTM C 876)

Half-cell potential, E (mV vs. C.S.E)	Corrosion condition
$-200 < E$	90 % probability of no corrosion
$-350 < E \leq -200$	an increasing probability of corrosion
$E \leq -350$	90 % probability of corrosion
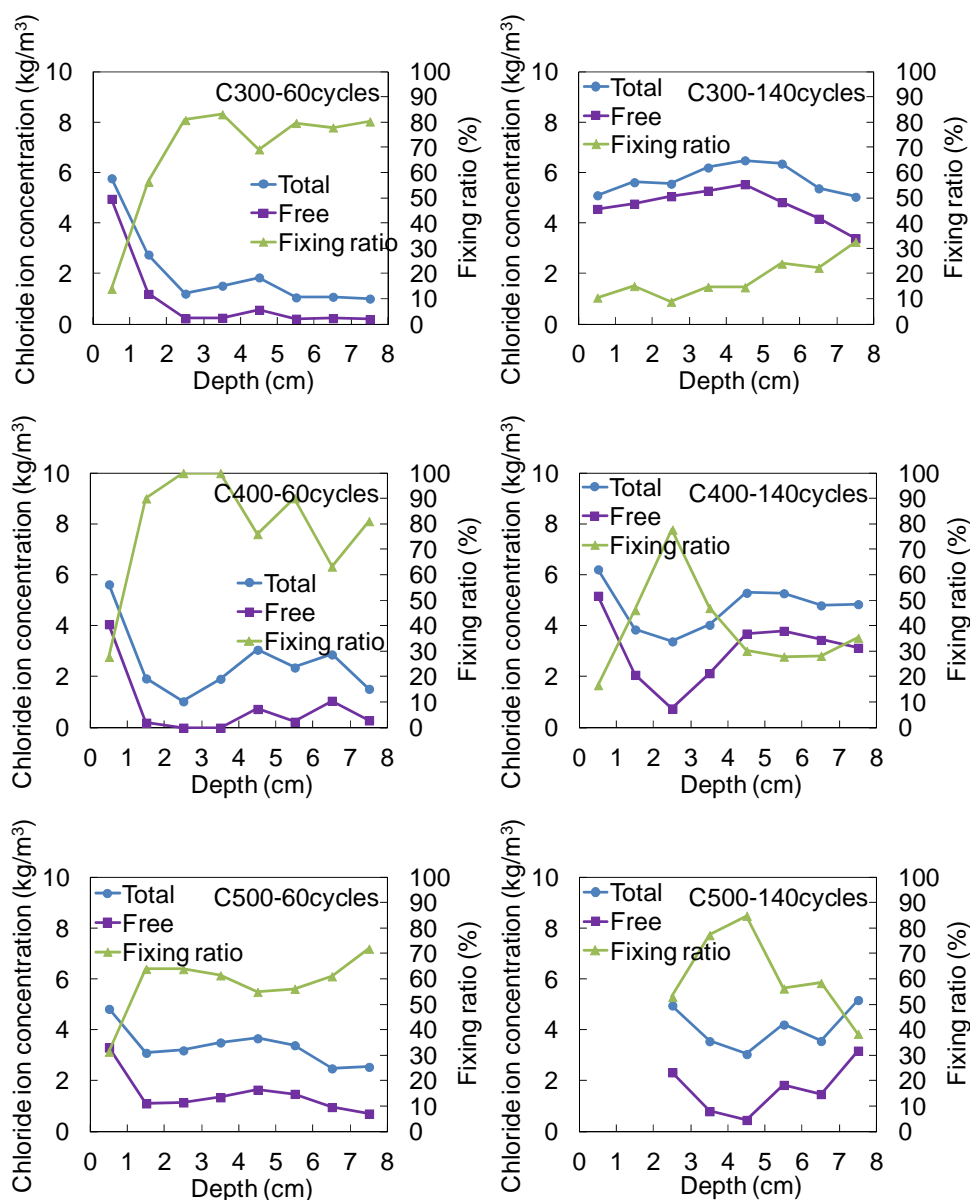
Figure 10. Distribution of chloride contents

At 60 cycles, C400 showed the highest fixing ratio. On the other hand, C500 showed the highest fixing ratio at 140 cycles. This is because large cement content in concrete can have high chloride binding capacities even when the specimen is subjected to freeze-thaw

cycles.   However, the fixing ratio tended to decrease when the FTC cycles increase or when measured at the deeper points, which might be indicating that freezing water in concrete possibly prevents the movement of chloride ion in concrete (Hashimoto, et al. 2012).

Concrete with more unit cement content showed less free chloride content, because the amount of fixed chloride content is determined by unit cement content (Kono, et al. 2006). In the other words, more unit cement content also showed higher fixing ratio in this study.

CONCLUSIONS

Concrete subjected to under freezing and thawing shows such characteristics that more unit cement content makes the fixing ratio of chloride content higher, which is the same as that under normal condition.   Therefore, more unit cement content concrete has less free chloride content under freezing and thawing condition.   As the results in this study, however, it is important to evaluate chloride penetration with considering a decrease in concrete cover particularly in the case that scaling occurs seriously.

ACKNOWLEDGEMENT

REFERENCES

ASTM C 672. *Standard Test Method for Scaling Resistance of Concrete Surfaces Exposed to Deicing Chemicals.*

ASTM C 876. *Standard Test Method for Corrosion Potentials of Uncoated Reinforcing Steel in Concrete.*

Hashimoto, K., Yokota, H., Sato, Y. and Sugiyama, T. (2012). "Chloride Ion Binding Behavior of Deicing Chlorides under Freeze-Thaw Environment." *Proc. of the 2nd International Conference on Microstructure Related Durability of Cementitious Composites*, 30.

Hayashida, H., Hama, Y., Taguchi, F. and Endo, H. (2010). "A Study on Temperature and Humidity Changes of Concrete Structures and the Prediction of Their Frost Deterioration." *Monthly Report of Civil Engineering Research Institute for Cold Region*, 687, 21-29.

Ishida, T., Miyahara, S. and Maruya, T. (2007). "Cl Binding Capacity of Mortars Made with Various Portland Cements and Mineral Admixtures." *Journal of JSCE*, 63 (1), 14-26.

JIS A 1154 (2012). *Methods of test for chloride ion content in hardened concrete.*

Kamata, E. (1988). "Frost damage and pore structure of concrete." *Proceedings of the Japan Concrete Institute*, 10 (1), 51-60.

Kono, K., Yamada, K., Hosokawa, Y. and Yang, S. (2006). "Chloride Threshold Contents for Steel Corrosion in Concrete with Various Cement Contents." *Proc. of the Concrete Structure Scenarios, JSMS*, 6, 267-274.

Kono, K., Ichikawa, M., Yang, S., Um, T. and Lee, J. (2010). "Threshold Chloride Contents and Regulations against Steel Corrosion in Concrete." *Journal of Research of the Taiheiyo Cement Corporation*, 158, 4-12.

Otsuki, N., Maruyama, S., Nishida, T. and Baccay, M. A. (2004). "Influence of Temperature on Corrosion Rate of Steel Bar in Carbonated Concrete Members." *Journal of The Society of Materials Science, Japan*, 54 (1), 108-113.